Retinal Nerve Fiber Layer Imaging with Spectral-domain Optical Coherence Tomography

Patterns of Retinal Nerve Fiber Layer Progression

Christopher Kai-Shun Leung, MB ChB, MD,[1] Marco Yu, BSc,[1] Robert N. Weinreb, MD,[2] Gilda Lai, BSc,[1] Guihua Xu, BM,[1] Dennis Shun-Chiu Lam, MD, FRCOphth[1]

Objective: To examine the use of the retinal nerve fiber layer (RNFL) thickness map generated by a spectral-domain optical coherence tomography (OCT) to detect RNFL progression and identify the pattern of progressive changes of RNFL defects in glaucoma.

Design: Prospective, longitudinal study.

Participants: One hundred eighty-six eyes of 103 glaucoma patients.

Methods: Patients were followed at 4-month intervals for ≥36 months for RNFL imaging and visual field examination. Both eyes were imaged by the Cirrus HD-OCT (Carl Zeiss Meditec Inc., Dublin, CA) and had visual field testing at the same visits. We defined RNFL progression by Guided Progression Analysis (Carl Zeiss Meditec) of serial RNFL thickness maps. The pattern of RNFL progression was evaluated by comparing the baseline RNFL thickness deviation map and the RNFL thickness change map. Visual field progression was defined by trend analysis of visual field index and event analysis based on the Early Manifest Glaucoma Trial criteria.

Main Outcome Measures: The presence and the pattern of RNFL progression.

Results: A total of 2135 OCT images were reviewed. Twenty-eight eyes (15.1%) from 24 patients (23.3%) had RNFL progression detected by RNFL thickness map analysis. Three RNFL progression patterns were observed: (1) widening of RNFL defects (24 eyes, 85.7%), (2) deepening of RNFL defects (2 eyes, 7.1%, both had concomitant widening of RNFL defects), and (3) development of new RNFL defects (5 eyes, 17.9%). The inferotemporal meridian (324°–336°) 2.0 mm away from the optic disc center was the most frequent location where RNFL progression was detected. Thirteen eyes (46.4%) had concomitant visual field progression; 61.5% (n = 8) of these had RNFL progression that preceded or occurred concurrently with visual field progression. Forty-two eyes from 37 patients (22.6%) had visual field progression by trend and/or event analyses without progression in the RNFL thickness map.

Conclusions: Analysis of serial RNFL thickness maps generated by the spectral-domain OCT facilitates the detection of RNFL progression in glaucoma.

Financial Disclosure(s): Proprietary or commercial disclosure may be found after the references. *Ophthalmology 2012;119:1858–1866 © 2012 by the American Academy of Ophthalmology.*

With a low test–retest variability,[1-3] spectral-domain optical coherence tomography (OCT) has been shown to be useful to detect progressive loss of the retinal nerve fiber layer (RNFL) in glaucoma patients.[4] Scanning the retina at a speed of 27 000 A-scans per second, the Cirrus HD-OCT (Carl Zeiss Meditec, Dublin, CA) can capture the RNFL thickness distribution profile in a map of 6×6 mm^2 around the optic disc (the RNFL thickness map) in 1.48 seconds. Yet, all previous spectral-domain and time-domain OCT studies investigating RNFL progression only reported measurements derived from a circle scan (3.4 mm in diameter centered at the optic disc).[4-10] Progressive changes in the spatial topology of RNFL defects in glaucoma have not been examined with the OCT technology.

Guided progression analysis (GPA) was introduced in 2009 (ver. 4.0) to facilitate topographic analysis of RNFL progression. By tracking RNFL changes with serial, registered RNFL thickness maps, GPA compares RNFL thickness of individual pixels between the baseline and follow-up images and provides a visual display of the area and location of significant change. Following RNFL progression in a topology map is expected to be an effective approach to detect the presence of and discern the pattern of RNFL progression. The objective of this study was to examine the

ISSN 0161-6420/12/$–see front matter
http://dx.doi.org/10.1016/j.ophtha.2012.03.044

use of the RNFL thickness map in detecting RNFL progression and identifying the progression patterns of RNFL defects in a group of glaucoma patients who had been followed prospectively every 4 months for ≥3 years with spectral-domain OCT RNFL imaging.

Methods

Subjects

A total of 103 glaucoma patients were consecutively enrolled and followed from June 2007 to January 2012 at the University Eye Center, the Chinese University of Hong Kong. They were enrolled for the study "Evaluation of RNFL Progression in Glaucoma," which was designed to investigate the roles of RNFL imaging for following glaucoma. All subjects underwent a full ophthalmic examination including measurement of visual acuity, refraction and intraocular pressure, gonioscopy, and fundus examination. Eyes were included if the visual acuity was ≥20/40. Eyes were excluded if there was evidence of macular disease, refractive or retinal surgery, or neurologic disease. Eyes were not excluded if they underwent cataract extraction and/or glaucoma filtration surgery during the study period. Glaucoma patients were identified based on the presence of visual field defects (described below) with corresponding optic disc and RNFL changes in ≥1 eye. Both eyes were imaged with Cirrus HD-OCT (Carl Zeiss Meditec) and examined by standard automated white-on-white perimetry (SITA Standard 24-2, Humphrey Field Analyzer II-i, Carl Zeiss Meditec) in the same visit every 4 months for ≥36 months. Visual fields and OCT images were assessed independently with masking of other clinical information. The study was conducted in accordance with the ethical standards stated in the 1964 Declaration of Helsinki and approved by local research ethics committee with informed consent obtained.

Visual Field Examination

A visual field was defined as reliable when fixation losses and false-positive and -negative errors were <20%. Average visual field sensitivity was expressed in visual field index (VFI) and mean deviation (MD), as calculated by the perimetry software. A visual field defect was defined as having ≥3 significant ($P<0.05$), nonedge, contiguous points with ≥1 at the $P<0.01$ level on the same side of the horizontal meridian in the pattern deviation plot and confirmed with ≥2 consecutive examinations. Seven visual fields were excluded because of fixation losses >20%, 6 were excluded because of false-positive errors >20%, and 4 were excluded because of false-negative errors >20%.

Visual field progression was defined with reference to the GPA (Carl Zeiss Meditec). The GPA reports results of both trend and event analyses. For trend analysis, progression was defined when there was a significant, negative trend between VFI and age. For event analysis, progression was defined according to the Early Manifest Glaucoma Trial criteria.[11] "Possible progression" signifies ≥3 points that have shown significant change from baseline in 2 consecutive tests, whereas "likely progression" signifies ≥3 points that have shown significant change from baseline in 3 consecutive tests. In this study, visual field progression was defined when there was a significant negative trend detected in the trend analysis and/or "possible progression" or "likely progression" in the event analysis.

Retinal Nerve Fiber Layer Imaging

Pupils were not routinely dilated during RNFL imaging. However, dilation with tropicamide and phenylephrine (0.5% each) was performed when the pupil size was too small to obtain images with the required quality. Only images with a signal strength of ≥6 were included in the analysis. Saccadic eye movement was detected with the line-scanning ophthalmoscope overlaid with OCT en face during OCT imaging. Images with motion artifact, poor centration, poor focus, or missing data were detected by the operator at the time of imaging with rescanning performed in the same visit. Ten images were excluded because of a signal strength of <6.

Spectral-domain OCT imaging was performed with the Cirrus HD-OCT (Carl Zeiss Meditec; software version 5.0). The acquisition rate of the Cirrus HD-OCT was 27 000 A-scans per second and the transverse and axial resolutions were 15 and 5 μm, respectively. An "optic disc cube" scan protocol was used to measure the RNFL thickness in a 6×6-mm^2 area and an RNFL thickness map was generated (Fig 1B).

Thickness Deviation and Change Maps

The RNFL thickness deviation and the RNFL thickness change maps were generated automatically from the OCT instrument (software version 5.0) and exported to a computer for analysis of the progression pattern of RNFL defects. The RNFL defects were visualized in the RNFL thickness deviation map, which was composed of 50×50 pixels (Fig 1C). A pixel is coded in yellow or red if the RNFL measurement was below the lower 95% and 99% of the centile ranges for that particular pixel, respectively. Only RNFL defects with a size >10 pixels coded in red or yellow in the RNFL thickness deviation map were analyzed in this study (an arbitrary criteria to exclude potential nonspecific changes detected in the RNFL thickness deviation map).

The RNFL thickness change map is a component of the GPA (Carl Zeiss Meditec), which provides an event-based analysis of RNFL progression based on serial RNFL thickness maps (Fig 1D). The software automatically aligned and registered baseline and follow-up OCT images so that the same pixel locations could be measured for change. The difference in RNFL thickness of an individual pixel between the baseline and the follow-up RNFL thickness maps was compared with an estimate of test–retest variability of that particular pixel (in-house proprietary database from Carl Zeiss Meditec). Pixels with RNFL thickness difference exceeding the test–retest variability between a follow-up and the first and the second baseline images are coded in yellow. If the same changes were evident in an additional follow-up image, the pixels are coded in red.

Evaluation of Progression Patterns

To investigate the progression patterns of RNFL defects, the RNFL thickness deviation map obtained at the baseline visit was overlaid with the RNFL thickness change map in the follow-up visits using a computer program written in Matlab R2010a (The MathWorks, Inc., Natick, MA) with reference to the retinal vessels trajectories (Fig 2, available at http://aaojournal.org). The pattern of progression was identified by comparing the first baseline RNFL thickness deviation map and the first and the final RNFL thickness change maps showing significant change, which had been confirmed with ≥2 consecutive follow-up examinations (pixels coded in red). Three RNFL progression patterns were identified. First, widening of RNFL defects was defined as the presence of significant change confirmed with ≥2 consecutive follow-up visits (red pixels in the RNFL thickness change map) within 2

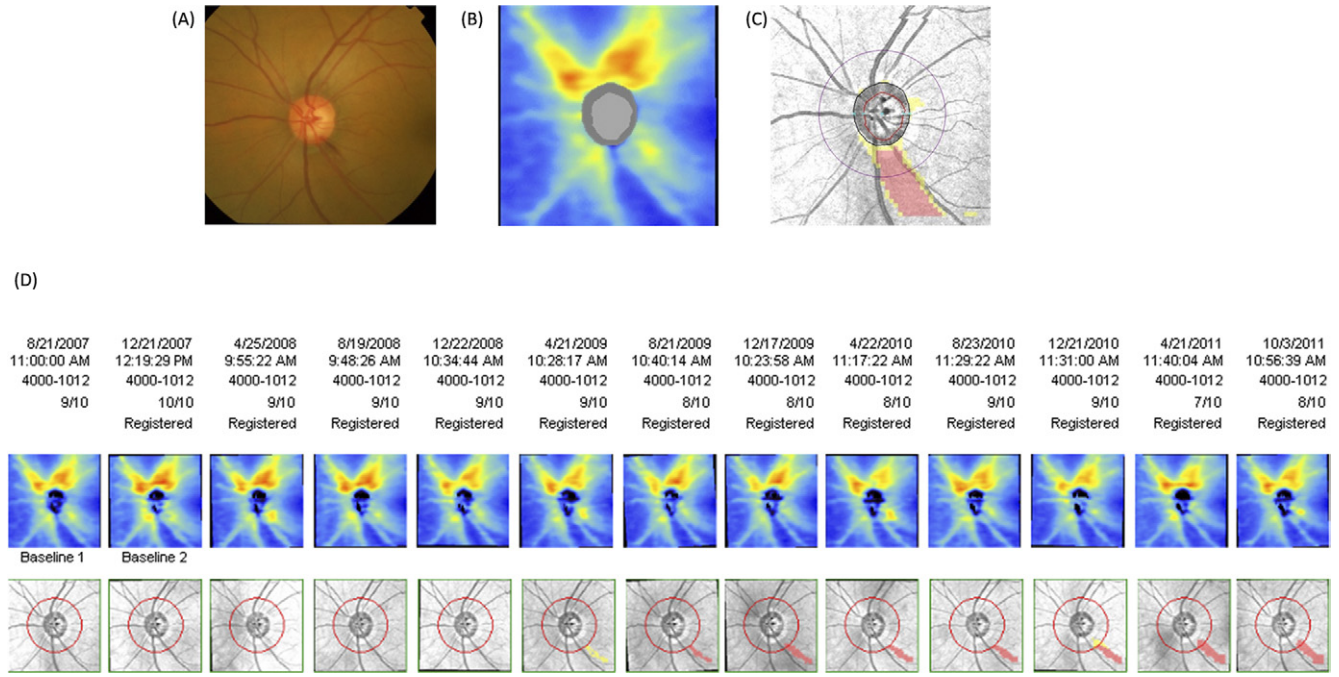

Figure 1

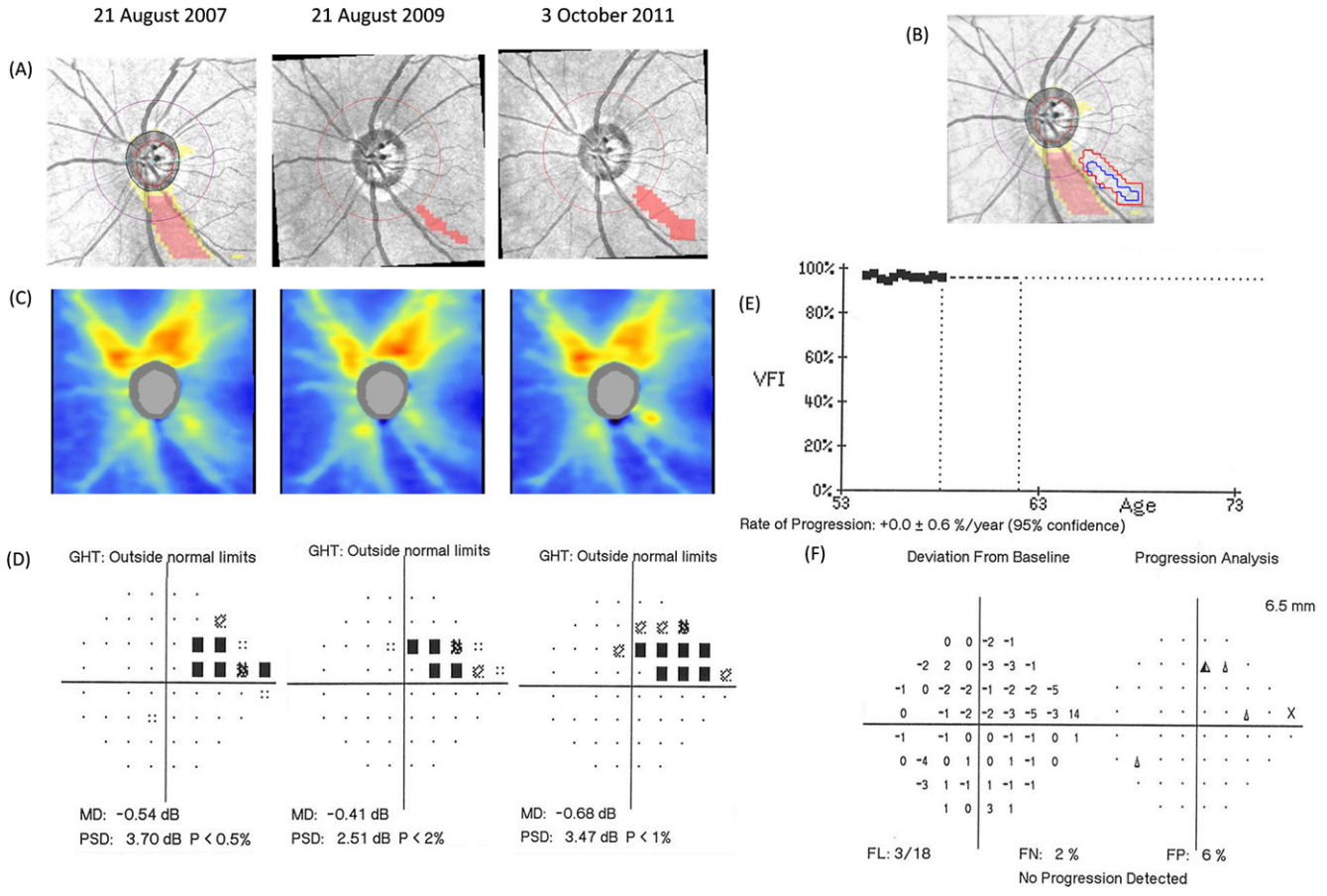

Figure 3

pixels to the edges of preexisting defects (yellow or red pixels detected in the RNFL thickness deviation map; Fig 3). Second, deepening of RNFL defects was defined as the presence of significant change confirmed with ≥2 consecutive follow-up visits overlapping with the preexisting defects for ≥10 pixels (Fig 4). Third, development of new defects was defined as the presence of significant change >2 pixels away from the edges of any preexisting defects confirmed with ≥2 consecutive follow-up visits (Fig 5). The area of significant change in the RNFL thickness change map was measured automatically by a computer program written in Matlab R2010a (The MathWorks, Inc.).

Statistical Analysis

Statistical analyses were performed using R 2.13.0 (R Foundation, Vienna, Austria). Differences in VFI, MD, average RNFL thickness at the baseline and the final follow-up visit were compared with linear mixed models after adjustment of correlation between fellow eyes. Comparison of average RNFL thickness, MD, and VFI among different patterns of RNFL progression was performed with the Kruskal–Wallis test.

Results

A total of 2135 OCT images from 186 eyes of 103 glaucoma patients prospectively followed for ≥36 months (mean follow-up, 44) were reviewed. The mean interval of OCT examination was 4.2 months and the average number of OCT images reviewed for each eye was 11.5. Of the eyes included, 53.2%, 17.7%, and 29.0% had mild (MD ≥ −6 dB), moderate (−6 dB > MD > −12 dB), or advanced glaucoma (MD ≤ −12 dB), respectively, as classified by the visual field MD[12] recorded at the baseline examination. There were significant differences in the average RNFL thickness, VFI, and MD between the baseline and the final visits (all $P \leq 0.001$). The demographics and visual field and RNFL measurements are presented in Table 1.

Guided progression analysis of the RNFL thickness maps detected 28 eyes (24 patients) with progression (15.1%, 28/186). Sixteen eyes (57.1%) had mild (MD ≥ −6 dB), 5 (17.9%) had moderate (−6 dB > MD > −12 dB), and 7 (25%) had advanced (MD ≤ −12 dB) visual field defects at the baseline visit. The mean duration between the first baseline RNFL thickness deviation map and the first RNFL thickness change map that had evidence of progression was 27 months. Three RNFL progression patterns were observed: (1) widening of RNFL defects (Fig 3), (2) deepening of RNFL defects (Fig 4), and (3) development of new RNFL defects (Fig 5). Twenty-four eyes (85.7%; 21 patients) showed widening of RNFL defects in which 17 (60.7%) widened toward the macula, 5 (17.9%) widened toward the nasal retina, 1 (3.6%) extended toward the superior retina, and 1 (3.6%) extended toward the inferior retina. Two eyes (7.1%; 2 patients) developed concomitant deepening of RNFL defects; no eye developed deepening of RNFL defects alone. Development of new RNFL defects was found in 5 eyes (17.9%; 5 patients), one of which showed concurrent widening of a preexisting RNFL defect. There were no differences in baseline average RNFL thickness, MD, or VFI among the 3 patterns of RNFL progression ($P \geq 0.283$). The area of significant change in the final RNFL thickness change map ranged between 0.338 and 3.238 mm^2 (mean, 1.039 mm^2). Progressive enlargement of RNFL defects, defined by the difference in area between the first and the final RNFL thickness change maps coded in red (difference in area outlined in blue [the first RNFL thickness change map] and red [the final RNFL thickness change map] in Figs 3B, 4B, and 5B), was found in 19 eyes (67.9%); the mean increase in RNFL defects area was 0.580 mm^2 (range, 0.032–1.604 mm^2) over a duration of 4 to 35 months (mean, 17 months).

Figure 6A shows the overlay of areas with RNFL progression evident in the final RNFL thickness change map (area coded in red in the RNFL thickness change map) of all the 28 progressing eyes after aligning the optic disc centers. RNFL progression was most frequently detected inferotemporally (324°–336°) at a distance of ~2.00 mm from the disc center. No RNFL progression was found at the nasal meridians (120°–210°). To identify the optimal size of the measurement circle for detection of RNFL progression, the mean number of progression events detected for each 10° of the measurement circle was plotted against different circle sizes with diameters ranged from 3.0 to 5.0 mm (calculation was performed every 0.1 mm; Fig 6B). There was a parabolic relationship between the frequency of progression detection and the size of the measurement circle. The peak was located at a 3.96- to 4.02-mm diameter measurement circle range.

Among the 28 eyes with RNFL progression, 13 (46.4%) also had visual field progression by trend analysis, event analyses. There were no differences in the proportion of eyes with visual field progression between eyes with widening of RNFL defects (45.8%) and eyes with development of new defects (40.0%; $P \geq 0.999$, Fisher exact test). The RNFL progression preceded (n =

←

Figure 1. (**A**) Optic disc photograph, (**B**) optical coherence tomography retinal nerve fiber layer (RNFL) thickness map, (**C**) RNFL thickness deviation map, and (**D**) guided progression analysis (GPA) printout of a glaucomatous eye with an inferotemporal RNFL defect. The RNFL thickness map (**B**) is a topology map (red signifies thick and blue signifies thin RNFL measurements) showing the RNFL distribution profile at the 6×6-mm^2 optic disc region. The RNFL thickness deviation map (**C**) indicates the pixels with abnormal RNFL thickness. A pixel would be coded in yellow or red if the RNFL measurement is below the lower 95% and 99% of the centile ranges for that particular pixel, respectively. The GPA (Carl Zeiss Meditec, Dublin, CA) printout shows serial RNFL thickness maps and RNFL thickness change maps of the same eye (**D**). Pixels with RNFL thickness difference exceeding the test–retest variability between a follow-up and the first and the second baseline images are coded in yellow. If the same changes are evident in an additional follow-up image, the pixels are coded in red. Significant progressive loss of the RNFL is noted at the inferotemporal sector.

←

Figure 3. Widening of retinal nerve fiber layer (RNFL) defects. An inferotemporal RNFL defect was detected in the baseline RNFL thickness deviation map (**A,** left panel) on August 21, 2007. Significant change in the RNFL thickness change map confirmed by 2 consecutive visits was first detected on August 21, 2009 (**A,** middle panel). Continuous enlargement of the defect was evident in the RNFL thickness map obtained in the latest follow-up visit (**A,** right panel). An overlay of the baseline RNFL thickness deviation map and the first (outlined in blue) and the latest (outlined in red) RNFL thickness change maps (**B**) shows that there is widening of the RNFL defect toward the macula. The corresponding RNFL thickness maps (**C**) and the visual field pattern deviation plots (**D**) are shown. Trend analysis of visual field index (VFI) (**E**) and event analysis based on the Early Manifest Glaucoma Trial criteria (**F**) indicate no visual field progression. FL = fixation loss; FN = false-negative; FP = false-positive; GHT = glaucoma hemifield test; MD = mean deviation; PSD = pattern standard deviation.

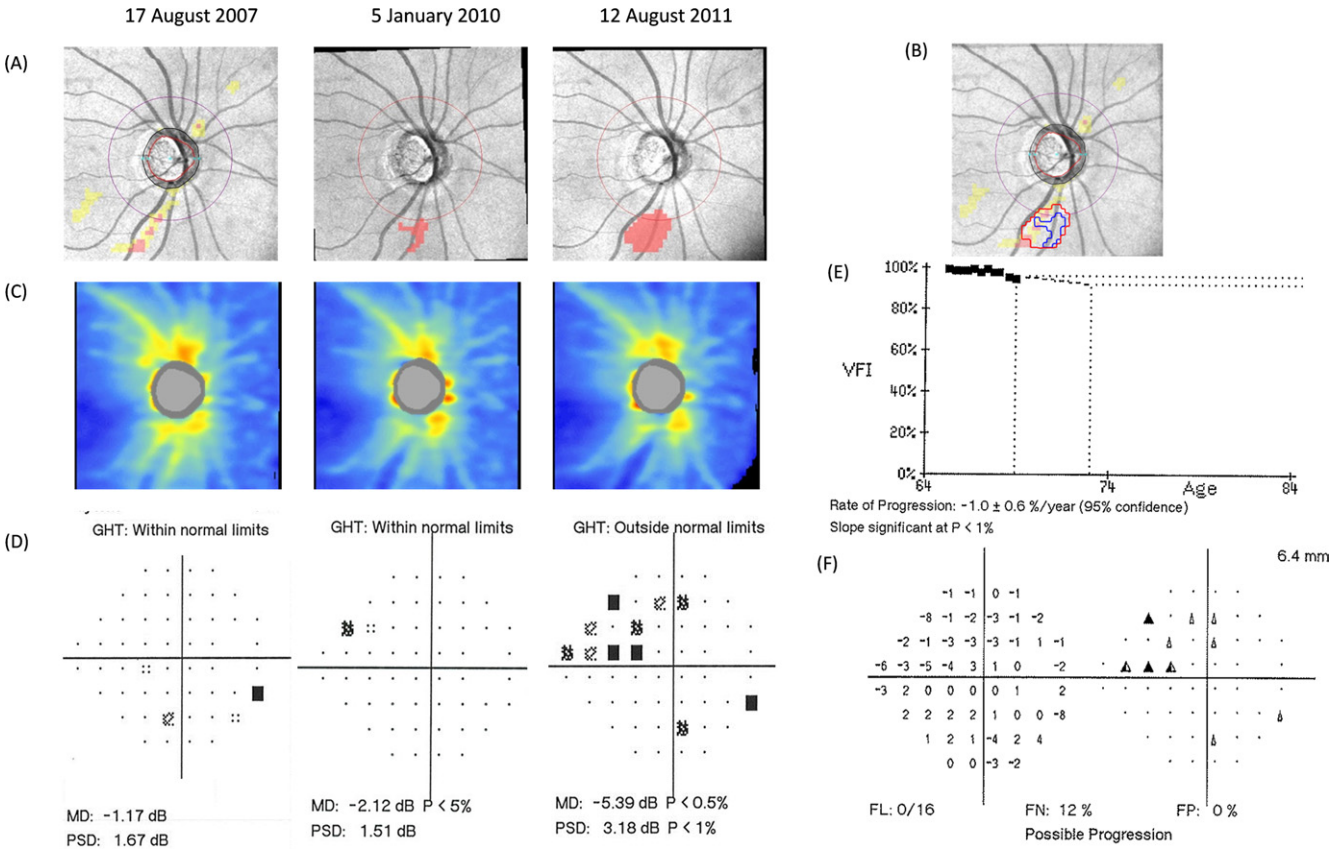

Figure 4. Deepening of retinal nerve fiber layer (RNFL) defects. An inferotemporal RNFL defect was detected in the baseline RNFL thickness deviation map (**A,** left panel) on August 17, 2007. Significant change in the RNFL thickness change map confirmed by 2 consecutive visits was first detected on January 5, 2010 (**A,** middle panel). Continuous enlargement of the defect was evident in the RNFL thickness map obtained in the latest follow-up visit (**A,** right panel). An overlay of the baseline RNFL thickness deviation map and the first (outlined in blue) and the latest (outlined in red) RNFL thickness change maps (**B**) shows that there is deepening of the RNFL defect as well as widening of the defect toward the nasal side. The corresponding RNFL thickness maps (**C**) and the visual field pattern deviation plots (**D**) are shown. Trend analysis of visual field index (VFI) (**E**) and event analysis based on the Early Manifest Glaucoma Trial criteria (**F**) indicate visual field progression. There is spatial correspondence between inferotemporal RNFL progression and superonasal visual field progression. FL = fixation loss; FN = false-negative; FP = false-positive; GHT = glaucoma hemifield test; MD = mean deviation; PSD = pattern standard deviation.

Figure 5. Development of new retinal nerve fiber layer (RNFL) defects. The fellow normal eye of a glaucoma patient had no definite RNFL defect (**A,** left panel; the superonasal RNFL defect in the baseline RNFL thickness deviation map is an artifact secondary to a vitreous opacity) and no visual field defect (**D,** left panel) at baseline on September 23, 2008. Significant change in the RNFL thickness change map confirmed by 2 consecutive visits was first detected on January 20, 2011 (**A,** middle panel). Continuous enlargement of the defect was evident in the RNFL thickness map obtained in the latest follow-up visit (**A,** right panel). An overlay of the baseline RNFL thickness deviation map and the first (outlined in blue) and the latest (outlined in red) RNFL thickness change maps is shown (**B**). The corresponding RNFL thickness maps (**C**) and the visual field pattern deviation plots (**D**) are shown (note the dark spot in the baseline RNFL thickness map—**C,** left panel—is a vitreous opacity). Trend analysis of visual field index (VFI) (**E**) and event analysis based on the Early Manifest Glaucoma Trial criteria (**F**) indicate no visual field progression, although an early superonasal visual field defect is already noted in the latest follow-up visit (**D,** right panel). FL = fixation loss; FN = false-negative; FP = false-positive; GHT = glaucoma hemifield test; MD = mean deviation; PSD = pattern standard deviation.

Figure 6. An overlay of areas with retinal nerve fiber layer (RNFL) progression evident in the final RNFL thickness change maps (area coded in red) of all the 28 progressing eyes after aligning the optic disc centers (**A**) and the frequency of progression detection measured at different circle sizes (**B**). RNFL progression was most frequently detected inferotemporally (324°–336°) at a distance of ~2.00 mm (range, 3.96–4.02 mm) away from the disc center. The inner circle has a diameter of 3.46 mm and the outer circle has a diameter of 4.00 mm. The color bar indicates the number of progression events. (**B**) The mean number of progression events detected for each 10° of the measurement circle was plotted against different circle sizes with diameters ranged from 3.0 to 5.0 mm (calculation was performed every 0.1 mm). The peak of progression detection was located at the size of 3.96- to 4.02-mm diameter circles. The 3.46-mm measurement circle would miss a considerable proportion of progressing eyes.

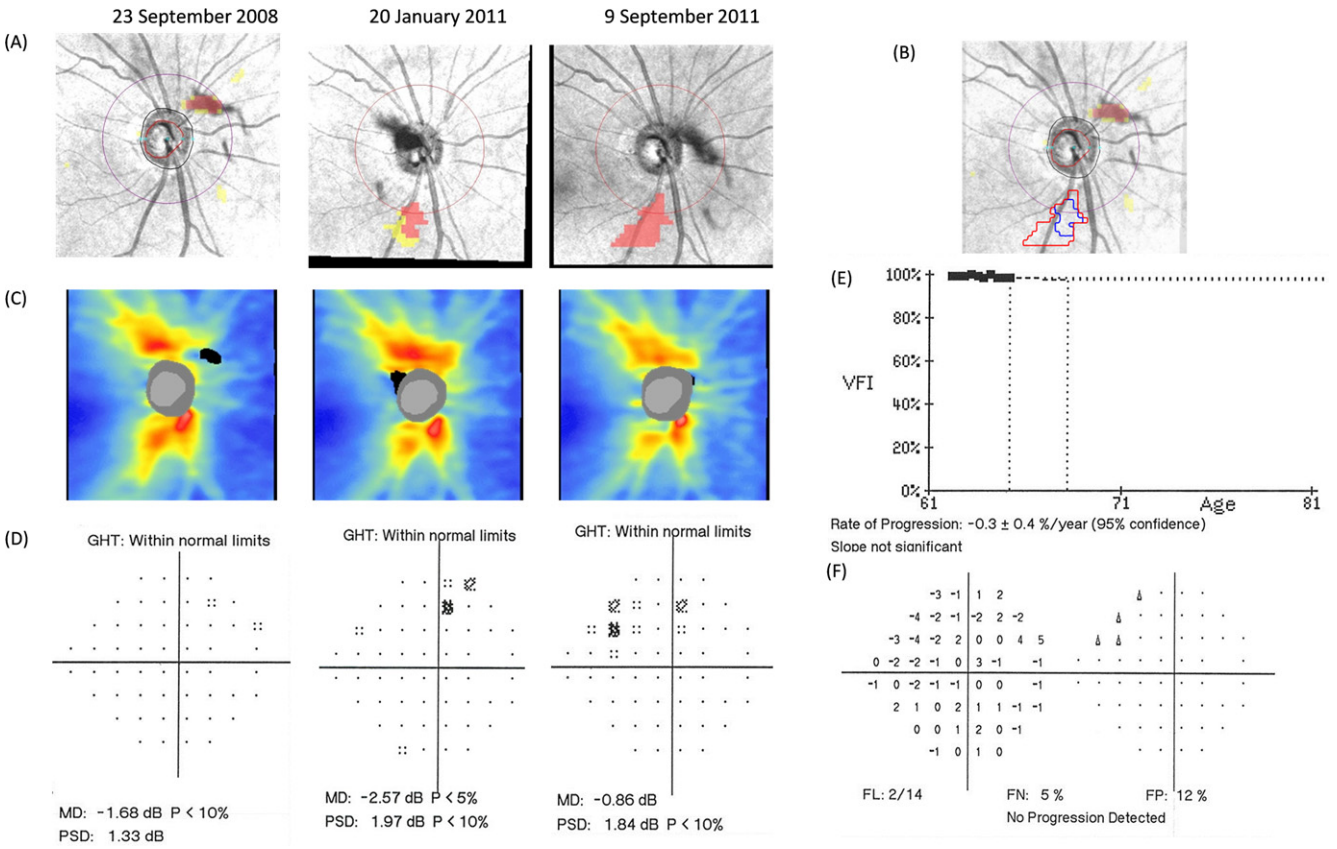

Figure 5

6) or occurred concomitantly (n = 2) with visual field progression in 8 of the 13 eyes (61.5%). For eyes with RNFL progression before visual field progression, the lag was between 4 and 28 months (mean, 12 months). Among the 13 eyes with visual field progression, 9 had progression by event analysis. All but 2 (77.8%, 7/9) showed spatial correspondence between RNFL and visual field progression (Fig 4F). There were 4 eyes with inferotemporal RNFL progression associated with superonasal visual field progression, 1 eye with superotemporal RNFL progression associated with inferonasal visual field progression, and 2 eyes with temporal RNFL progression extending to the papillomacular bundle associated with paracentral visual field progression.

Four eyes (14.3%) showed areas of RNFL thickness increase in the final RNFL thickness change map (mean, 0.462 mm^2; range, 0.282–0.746 mm^2). All were found over the temporal retina (330°–30°). The area of increase in RNFL thickness was signifi-

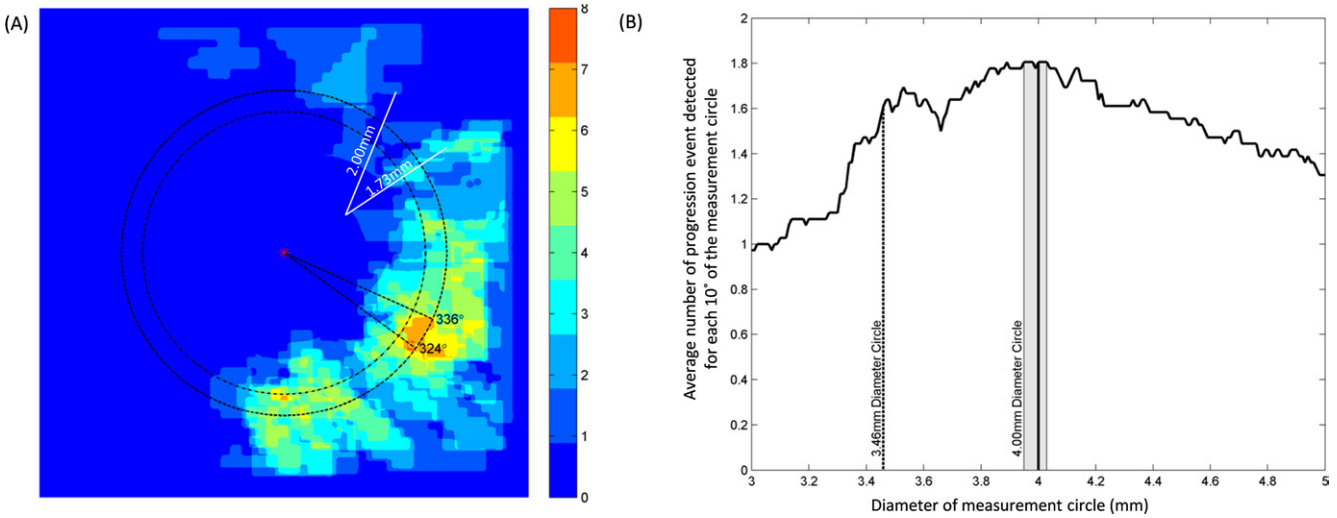

Figure 6

cantly smaller than the area of RNFL loss (mean, 1.039 mm^2; range, 0.338–3.238 mm^2) measured in the final RNFL thickness change map ($P<0.001$). Thirty-seven patients (42 eyes) had visual field progression by trend, event analyses, or both, without progression in the RNFL thickness map.

Discussion

To our knowledge, this is the first study demonstrating that it is feasible to track progressive RNFL changes and identify the pattern of RNFL progression using the RNFL thickness map generated by the spectral-domain OCT. Over a median follow-up period of 42 months, 28 eyes (15.1%) showed evidence of RNFL progression in the RNFL thickness map analysis. The most common pattern of RNFL progression was widening of RNFL defects (85.7%), which was followed by development of new RNFL defects (17.9%) and then deepening of RNFL defects (7.1%). The inferotemporal (324°–336°) meridian at a distance of ~2.0 mm away from the optic disc center was the most common location where RNFL progression was detected. The spectral-domain OCT RNFL thickness map analysis can provide an alternative to red-free RNFL photography for detecting the presence of and discerning the pattern of RNFL progression in glaucoma.

Studying the pattern of RNFL progression has been obfuscated by the fact that RNFL measurements derived from digital imaging instruments including OCT and scanning laser polarimetry have been largely limited to circumpapillary measurements. Although a number of studies have characterized the pattern of RNFL defects in glaucoma with red-free RNFL photography,[13-16] less is known about the progression pattern of RNFL defects. Suh et al[17] followed 65 glaucomatous eyes that had localized RNFL defects demonstrating evidence of RNFL progression on serial red-free RNFL photographs. They characterized 4 patterns of RNFL progression, including widening of RNFL defects toward the macula (56.9%), deepening of RNFL defects (38.5%), appearance of a new defect (9.2%), and widening of RNFL defects away from the macula (7.7%). Our finding of widening of RNFL defects toward the macula being the most common pattern of progression (60.7%) concurs with their results. However, we observed proportionately more eyes with development of new defects (17.9%) and proportionately fewer eyes with deepening of RNFL defects (7.1%). The discrepancy in the frequency distribution of the progression patterns between the studies is likely attributed to the fundamental differences between red-free photography and OCT in visualizing and analyzing RNFL defects. First, detecting the borders of RNFL defects with red-free photography is difficult in eyes with diffuse RNFL atrophy when the contrast is low. For this reason, only localized RNFL defects can be reliably examined for change as in the study by Suh et al, in which only eyes with localized RNFL defects were included in the study. By contrast, both localized and diffuse RNFL defects can be visualized in the OCT RNFL thickness deviation map.[18,19] By comparing the changes in the RNFL thickness maps, it is feasible to follow the pattern of RNFL progression independent of the severity of disease. Second, discerning deepening of RNFL defects is largely subjective with red-free photography and is defined based on textural changes in the appearance of RNFL striations.[15-17] Determining further reduction in RNFL thickness over a preexisting RNFL defect using red-free RNFL photographs is challenging. Analysis of thickness change in the OCT RNFL thickness map is more effective than subjective assessment of red-free RNFL photographs to detect RNFL thinning.

Table 1. Demographics, Visual Field, and Optical Coherence Tomography (OCT) Retinal Nerve Fiber Layer (RNFL) Measurements (Mean ± SD)

Total number of subjects	103
Total number of eyes	186
Gender (female/male)	39/64
Age (yrs)	51.1±14.0
Spherical error (D)	−2.65±3.98
Visual field measurement	
Total number of visual field tests	2117
Baseline MD (dB)	−8.52±8.41
Baseline VFI (%)	77.15±25.43
MD at the final visit (dB)	−9.81±8.46
VFI at the final visit (%)	74.96±26.33
Cirrus HD-OCT RNFL measurement	
Total number of OCT tests	2135
Baseline average RNFL thickness (μm)	70.27±13.13
Average RNFL thickness at the final visit (μm)	68.32±12.26

D = diopter; dB = decibel; MD = mean deviation; SD = standard deviation; VFI = visual field index.

That widening of RNFL defects is the predominate form of progression pattern (85.7%) suggests RNFL defects progress in a specific sequence. Defects in the RNFL usually initiate at the inferotemporal meridians and widen toward the macula—less often the nasal retina—before development of new defects at the opposite hemifield. The predilection for RNFL progression at the inferotemporal meridians agrees with the observation that the superonasal visual field is frequently affected and deteriorates faster as glaucoma progresses.[20] Yet, extension to the papillomacular bundle (the temporal 90°) is less common (Fig 6A) and usually occurs at the end stages of disease. The relative preservation of the papillomacular bundles aligns with the fact that central vision is well-preserved in glaucoma patients even when the loss in visual field is substantive. Discerning the pattern of RNFL progression not only offers important insights into the development and progression of glaucoma, but also provides prognostic information in management of glaucoma patients. For example, patients with progressive widening of RNFL defects toward the papillomacular bundles would need a closer follow-up and may need more aggressive treatment to prevent progressive loss of vision.

Although an RNFL thickness map analysis is preferable to circumpapillary measurement to identify the location of RNFL progression, measuring the average RNFL thickness and estimating its rate of change still relies on circle scans around the optic disc. In fact, RNFL thickness measurements in the analysis printout of both the spectral-domain and the time-domain OCT has been based on the 3.46-mm diameter circle scan since the introduction of OCT in the early 1990s. The adoption of a 3.46-mm diameter circle was

based on a landmark study comparing RNFL measurement reproducibility obtained from 3 circle diameters—2.9, 3.4, and 4.5 mm—using the first-generation time-domain OCT prototype, which showed that the 3.4-mm diameter circumpapillary measurement had greater intraclass correlation coefficients in both normal and glaucomatous eyes.[21] It was recommended that the measurement size of 3.4-mm diameter would be large enough to avoid overlap with the optic disc and allowed RNFL measurement in a thicker area than the 4.5-mm diameter circle.[21] With RNFL thickness map analysis, we provide preliminary evidence suggesting that RNFL progression would be best detected at a distance of ~2.00 mm away from the optic disc center. The 3.46-mm diameter circle misses a considerable proportion of progressing eyes (Fig 6A). Although it is largely unclear why this region exhibits a proclivity for RNFL progression, the ability to detect progression is likely dictated by the density of nerve fibers, which decreases with the distance away from the optic disc. Loss of the RNFL may not be readily detectable at regions close to the optic disc where the nerve fibers are densely packed. Likewise, RNFL reduction could be difficult to detect at regions where the RNFL is thin. Revising the circle size for progression analysis may be needed in the future OCT software upgrade.

It is not surprising to observe that <50% of eyes had concomitant RNFL and visual field progression because it has been long recognized that the agreement of progression detection between structure and function is poor.[4,5,22-24] An important reason for the poor agreement is related to the fact that glaucoma is a chronic disease and it often takes years to observe progression. Given a sufficiently long follow-up, it is expected that agreement of progression detection between structure and function would improve. With a median follow-up duration of 42 months, RNFL progression preceded or proceeded concurrently with visual field progression in a significant proportion of eyes (61.5%), showing progression in both structure and function. More important, in eyes with RNFL progression and visual field progression by event analysis (n = 9), we showed that 77.8% had spatial correspondence in the progression (spatial correspondence cannot be determined with trend analysis of VFI). These findings strengthen the notion that progression analysis with the RNFL thickness map is an effective approach to detect glaucoma progression and may provide prognostic information in predicting corresponding functional loss in glaucoma management.

The OCT RNFL thickness map analysis, however, is not without limitations. The GPA adopts an event-based approach to define change in the RNFL thickness map. The differences in RNFL thickness of individual pixels in the RNFL thickness map between the baseline and follow-up visits were compared with the test–retest variabilities derived from a built-in database comprising normal healthy subjects. Although the test–retest variabilities may not change with the severity of disease (there is no correlation between test–retest variability and RNFL thickness),[25] it is uncertain if the use of normal subjects' test–retest variabilities to define change in advanced glaucoma patients when the RNFL is thin would be as sensitive as in early glaucoma when the RNFL is relatively thick. The GPA may show widening of RNFL defects more readily (detecting change in thickness of pixels that are still within the normal limits) than deepening of RNFL defects (detecting change in thickness of pixels that are already outside the normal limits). Rather than using "group" test–retest variabilities, computing "individual" test–retest variabilities may improve the sensitivity to detect change. Further studies are needed to identify the optimal strategy to detect RNFL progression with the RNFL thickness map. Assuming RNFL thickness does not increase with time, an increase in RNFL thickness signifies measurement variability. With 14.3% of eyes showing an increase in RNFL thickness in the RNFL thickness map, the specificity of GPA can be considered moderately high. Notably, the area of increase in RNFL thickness was significantly smaller than the area of RNFL progression. Other limitations of the study include a relatively short follow-up period (mean, 44 months) and the lack of analysis investigating potential risk factors (e.g., intraocular pressure control) for RNFL progression (which would be addressed in a follow-up study).

In summary, studying the RNFL topology with the spectral-domain OCT RNFL thickness maps offers a useful alternative to red-free RNFL photography to detect RNFL defects and determine the pattern of RNFL progression with the added advantages of providing objective and quantitative analysis of change. Tracking the topographic changes of the RNFL can serve as a new paradigm to monitor the continuum of glaucoma progression.

References

1. Mwanza JC, Chang RT, Budenz DL, et al. Reproducibility of peripapillary retinal nerve fiber layer thickness and optic nerve head parameters measured with Cirrus HD-OCT in glaucomatous eyes. Invest Ophthalmol Vis Sci 2010;51:5724–30.
2. Kim JS, Ishikawa H, Sung KR, et al. Retinal nerve fibre layer thickness measurement reproducibility improved with spectral domain optical coherence tomography. Br J Ophthalmol 2009; 93:1057–63.
3. Leung CK, Cheung CY, Weinreb RN, et al. Retinal nerve fiber layer imaging with spectral-domain optical coherence tomography: a variability and diagnostic performance study. Ophthalmology 2009;116:1257–63.
4. Leung CK, Chiu V, Weinreb RN, et al. Evaluation of retinal nerve fiber layer progression in glaucoma: a comparison between spectral-domain and time-domain optical coherence tomography. Ophthalmology 2011;118:1558–62.
5. Leung CK, Liu S, Weinreb RN, et al. Evaluation of retinal nerve fiber layer progression in glaucoma: a prospective analysis with neuroretinal rim and visual field progression. Ophthalmology 2011;118:1551–7.
6. Leung CK, Cheung CY, Weinreb RN, et al. Evaluation of retinal nerve fiber layer progression in glaucoma: a comparison between the fast and the regular retinal nerve fiber layer scans. Ophthalmology 2011;118:763–7.
7. Lee EJ, Kim TW, Weinreb RN, et al. Trend-based analysis of retinal nerve fiber layer thickness measured by optical coherence tomography in eyes with localized nerve fiber layer defects. Invest Ophthalmol Vis Sci 2011;52:1138–44.
8. Lee EJ, Kim TW, Weinreb RN, et al. β-Zone parapapillary atrophy and the rate of retinal nerve fiber layer thinning in glaucoma. Invest Ophthalmol Vis Sci 2011;52:4422–7.

9. Leung CK, Cheung CY, Weinreb RN, et al. Evaluation of retinal nerve fiber layer progression in glaucoma: a study on optical coherence tomography guided progression analysis. Invest Ophthalmol Vis Sci 2010;51:217–22.
10. Medeiros FA, Zangwill LM, Alencar LM, et al. Detection of glaucoma progression with Stratus OCT retinal nerve fiber layer, optic nerve head, and macular thickness measurements. Invest Ophthalmol Vis Sci 2009;50:5741–8.
11. Heijl A, Leske MC, Bengtsson B, et al, EMGT Group. Measuring visual field progression in the Early Manifest Glaucoma Trial. Acta Ophthalmol Scand 2003;81:286–93.
12. Hodapp E, Parrish RK II, Anderson DR. Clinical Decisions in Glaucoma. St. Louis: Mosby; 1993:52–61.
13. Sommer A, Miller NR, Pollack I, et al. The nerve fiber layer in the diagnosis of glaucoma. Arch Ophthalmol 1977;95: 2149–56.
14. Tuulonen A, Airaksinen PJ. Initial glaucomatous optic disk and retinal nerve fiber layer abnormalities and their progression. Am J Ophthalmol 1991;111:485–90.
15. Sommer A, Quigley HA, Robin AL, et al. Evaluation of nerve fiber layer assessment. Arch Ophthalmol 1984;102:1766–71.
16. Quigley HA, Addicks EM. Quantitative studies of retinal nerve fiber layer defects. Arch Ophthalmol 1982;100:807–14.
17. Suh MH, Kim DM, Kim YK, et al. Patterns of progression of localized retinal nerve fibre layer defect on red-free fundus photographs in normal-tension glaucoma. Eye (Lond) 2010; 24:857–63.
18. Leung CK, Choi N, Weinreb RN, et al. Retinal nerve fiber layer imaging with spectral-domain optical coherence tomography: pattern of RNFL defects in glaucoma. Ophthalmology 2010; 117:2337–44.
19. Leung CK, Lam S, Weinreb RN, et al. Retinal nerve fiber layer imaging with spectral-domain optical coherence tomography: analysis of the retinal nerve fiber layer map for glaucoma detection. Ophthalmology 2010;117:1684–91.
20. Pereira ML, Kim CS, Zimmerman MB, et al. Rate and pattern of visual field decline in primary open-angle glaucoma. Ophthalmology 2002;109:2232–40.
21. Schuman JS, Pedut-Kloizman T, Hertzmark E, et al. Reproducibility of nerve fiber layer thickness measurements using optical coherence tomography. Ophthalmology 1996;103:1889–98.
22. Wollstein G, Schuman JS, Price LL, et al. Optical coherence tomography longitudinal evaluation of retinal nerve fiber layer thickness in glaucoma. Arch Ophthalmol 2005;123:464–70.
23. Strouthidis NG, Scott A, Peter NM, Garway-Heath DF. Optic disc and visual field progression in ocular hypertensive subjects: detection rates, specificity, and agreement. Invest Ophthalmol Vis Sci 2006;47:2904–10.
24. Artes PH, Chauhan BC. Longitudinal changes in the visual field and optic disc in glaucoma. Prog Retin Eye Res 2005; 24:333–54.
25. Leung CK, Cheung CY, Lin D, et al. Longitudinal variability of optic disc and retinal nerve fiber layer measurements. Invest Ophthalmol Vis Sci 2008;49:4886–92.

Footnotes and Financial Disclosures

Originally received: November 29, 2011.
Final revision: March 24, 2012.
Accepted: March 26, 2012.
Available online: June 5, 2012. Manuscript no. 2011-1710.

[1] Department of Ophthalmology and Visual Sciences, The Chinese University of Hong Kong, Hong Kong, PRC.

[2] Hamilton Glaucoma Center and the Department of Ophthalmology, University of California, San Diego, California.

Financial Disclosure(s):
The authors have made the following disclosures: Christopher Kai-Shun Leung, Speaker honorarium, Carl Zeiss Meditec, Heidelberg Engineering; Research support, Carl Zeiss Meditec, Optovue. Robert N. Weinreb, Consultant, Optovue, Carl Zeiss Meditec; Research support, Carl Zeiss Meditec, Heidelberg Engineering, Optovue, Topcon, Nidek.

Supported by a research grant from the Chinese University of Hong Kong (Direct Grant 2010-2011).

Correspondence:
Christopher Leung, Department of Ophthalmology and Visual Sciences, The Chinese University of Hong Kong, Hong Kong, PRC. E-mail: tlims00@hotmail.com.